Biosynthesis of Silver Nanoparticles Using Orange Peel Extract for Application in Catalytic Degradation of Methylene Blue Dye

Cathleen Simatupang[1], Vinod K Jindal[2], and Ranjna Jindal[1*]

[1]*Department of Civil and Environmental Engineering, Faculty of Engineering, Mahidol University, Nakhon Pathom 73170, Thailand*
[2]*Department of Chemical Engineering, Faculty of Engineering, Mahidol University, Nakhon Pathom 73170, Thailand*

ARTICLE INFO

Received: 12 May 2021
Received in revised: 8 Jul 2021
Accepted: 12 Jul 2021
Published online: 25 Aug 2021
DOI: 10.32526/ennrj/19/202100088

Keywords:
Biosynthesis/ Orange peel extract/ Silver nanoparticles/ Central composite design/ Methylene blue dye

*** Corresponding author:**
E-mail: ranjna.jin@mahidol.ac.th

ABSTRACT

Interest in the biosynthesis of silver nanoparticles (AgNPs) has been steadily increasing primarily due to their numerous applications in various fields, low-cost, use of non-toxic environmentally-friendly materials and easy implementation. This study focused on the biosynthesis of AgNPs using orange peel extract (OPE), optimization of process conditions, and application in catalytic degradation of methylene blue (MB) dye used in the textile industry. A central composite design in response surface methodology resulted in optimum conditions of 0.0075 g dry peel/mL for OPE concentration, pH of 11 and 1.5 mM silver nitrate concentration. The optimum conditions for the response variables corresponded to the peak absorbance of 0.79 and SPR wavelength of 403.8 nm in UV-vis spectra, and minimum particle size of 12.9 nm. In addition, peak absorbance and SPR wavelength appeared to be related to the size of the AgNPs. A full-factorial design for the catalytic degradation of MB dye by the biosynthesized AgNPs for 1 h indicated the maximum influence of AgNPs compared to the concentrations of MB dye and $NaBH_4$ in decreasing order. The MB dye was reduced rapidly with $NaBH_4$ in the presence of AgNPs due to their catalytic action. The findings of the study show the potential of OPE for the biosynthesis of AgNPs with excellent catalytic activity for the treatment of MB dye in industrial effluent.

1. INTRODUCTION

Dyes are a major class of synthetic organic compounds released by many industries including paper, plastic, leather, food, and cosmetics. (Husain, 2010; Zollinger, 1987). Methylene blue (MB) is widely used in manufacturing of paints and printing inks, paper and plastics (Nasuha et al., 2010). Dyes lead to the formation of harmful by-products in industrial wastewater that ultimately cause significant damage to the aquatic environment (Sabouri et al., 2020). Conventional water treatment methods are not very effective for the degradation of dyes due to their stable and complex structure. Therefore, new techniques are needed to remove such contaminants from the wastewater or convert them into harmless products.

Nanotechnology has attracted much interest due to the wide range of potential applications such as catalysis, imaging, biological product development, drug delivery, antimicrobial activity, and pollution prevention. (Khodadadi et al., 2017; Ndolomingo et al., 2020; Jamkhande et al., 2019). Among a large number of materials used in nanotechnology, silver nanoparticles (AgNPs) have gained prominence due to their excellent properties and good catalytic activity (Bhattarai et al., 2018; Rostami-Vartooni et al., 2016) and can be synthesized by physical, chemical, and biological methods (Xu et al., 2020; Shanmuganathan et al., 2019). Biological methods are considered superior to the physical and chemical methods due to their simplicity, low cost and eco-friendliness (Patil et al., 2012; Menon et al., 2019).

The biosynthesis of AgNPs using plant extracts both as reducing and stabilizing agents offers distinct advantages of nontoxicity, simplicity, and cost-effectiveness (Ahmad et al., 2019; Zhang et al., 2020). The effects of parameters such as plant extract concentration, silver nitrate ($AgNO_3$) concentration,

Citation: Simatupang C, Jindal VK, Jindal R. Biosynthesis of silver nanoparticles using orange peel extract for application in catalytic degradation of methylene blue dye. Environ. Nat. Resour. J. 2021;19(6):468-480. (https://doi.org/10.32526/ennrj/19/202100088)

temperature, and time on the biosynthesized AgNPs have been studied using the response surface methodology (RSM) (Heydari and Zaryabi, 2018; Biswas and Mulaba-Bafubiandi, 2016; Chinnasamy et al., 2017; Nikaeen et al., 2020).

The application of AgNPs in catalytic dye degradation has been reported in the presence of $NaBH_4$ (Bonnia et al., 2016; Indana et al., 2016; Saha et al., 2017; Suvith and Philip, 2014) and when used alone (Vanaja et al., 2014; Bhakya et al., 2015; Jyoti and Singh, 2016; Vidhu and Philip, 2014). The size of AgNPs appears to affect their catalytic activity in dye degradation (Suvith and Philip, 2014; Jana et al., 2000).

Orange is a popular citrus fruit product with a global production of about 48.8 million tons in 2015-2016 (Bátori et al., 2017). In Thailand, tangerine is the most important type of citrus fruit contributing about 76% of total production (Sethpakdee, 1997). Orange peels are rich in alcoholic compounds, flavonoids and proteins (Ozturk et al., 2018; Gupta et al., 2014) and thus orange peel extract (OPE) can reduce Ag^+ and stabilize AgNPs (Kaviya et al., 2011; Kahrilas et al., 2014; Saratale et al., 2018).

The information on the biosynthesis of AgNPs using OPE for catalytic degradation of MB dye based on the design of experiments in RSM, to our knowledge, has not been reported. Therefore, the overall objective of this study was to determine the optimum conditions for the biosynthesis of AgNPs with OPE using a central composite design (CCD) in RSM for application in catalytic degradation of MB dye. Subsequently, the relative significance of the process parameters in catalytic dye degradation was investigated using a full-factorial design.

2. METHODOLOGY

2.1 Orange peel extract preparation

Fresh orange peels were washed with distilled water, cut into small pieces, and oven dried at 93°C for 60 min. A blender was used to produce fine powder passing through a 20-mesh screen. A 5 g sample of dried peel was mixed with 100 mL of distilled water at 60ºC using a magnetic stirrer for 10 min. The peel extract was subsequently cooled, filtered and stored at 4°C until further use. The concentration of OPE was expressed as g dry peel/mL.

2.2 Biosynthesis of AgNPs

A 10 mM stock solution of $AgNO_3$ (analytical grade, Sigma-Aldrich) in deionized water (DI) and OPE with 0.05 g/mL concentration were prepared in advance, and diluted to produce AgNPs as needed. The pH of OPE was adjusted using 1 mM KOH solution prior to the addition of $AgNO_3$ solution and DI water according to the experimental design to make up the 20 mL volume. All experiments were carried out at room temperature under bright day light conditions.

2.3 AgNPs Characterization

The AgNPs in suspension were characterized by a UV-vis spectrophotometer (GENESYS 10s) in the 350-550 nm range for peak absorbance and characteristic surface plasmon resonance (SPR) wavelength. The baseline spectra were obtained for the OPE at specific concentrations used in the tests. A dilution factor of 50 was used to determine UV-vis spectra of all test samples. The size distribution of AgNPs was determined by dynamic light scattering (DLS) using Malvern Zetasizer 7 based on 10 repeated measurements.

2.4 Catalytic dye degradation

Stock solutions of 10 mM MB dye and 1 M $NaBH_4$ were prepared and diluted as needed. The chemicals used were of analytical grade. The dye degradation was investigated for 1 h in a 20 mL mixture prepared by adding MB dye, $NaBH_4$, AgNPs solutions and DI water based on the reduction in absorbance at a 663 nm wavelength in the UV-vis spectra using the following equation (Raj et al., 2020).

$$\text{Dye degradation (\%)} = \frac{A_0 - A_t}{A_0} \times 100\ \% \qquad (1)$$

Where; A_0 is absorbance of the MB dye solution at the start of experiment and A_t is the absorbance after reaction time t, respectively.

Additional experiments were performed to identify the individual and combined effects of 1 mM $NaBH_4$ and 1 mL AgNPs solutions on the reduction of 0.5 mM MB dye for 180 min by adjusting the sample volume to 20 mL with DI water.

2.5 Experimental design

In the biosynthesis of AgNPs, the independent variables included OPE concentration, $AgNO_3$ concentration, and pH, while AgNPs size, peak absorbance, and SPR wavelength represented response variables. A central composite design (CCD) with eight factorial, six axial and six center point

experimental runs was used. The coded and actual values of independent variables and their levels are shown in Table 1.

In dye degradation, the effect of initial dye concentration, $NaBH_4$ concentration, and the volume of AgNPs solution was investigated using a full-factorial design with eight factorial and two center point experiments. Table 2 shows the coded and actual values of each variables.

Table 1. Coded and actual values of independent variables for the biosynthesis of AgNPs.

Variables	Coded levels				
	-1.682	-1	0	1	1.682
OPE conc. (X_1) (g/mL)	0.0008	0.0025	0.005	0.0075	0.0092
pH (X_2)	5.64	7	9	11	12.4
$AgNO_3$ conc. (X_3) (mM)	0.16	0.5	1	1.5	1.84

Table 2. Coded and actual values for dye degradation.

Variables	Coded levels		
	-1	0	1
Dye Conc. (X_1) (g/mL)	0.000031985	0.0001759	0.00031985
$NaBH_4$ (X_2) (mM)	1	5.5	10
AgNPs conc. (X_3) (mM)	0.1	0.5	0.9

All experiments were replicated twice and the mean value of the response was used in statistical analysis for developing the models.

2.6 Statistical analysis

A second-order polynomial model (Equation 2) was fitted to experimental data using regression analysis in MS Excel.

$$Y = \beta_0 + \sum_{i=1}^{3} \beta_i . X_i + \sum_{i=1}^{3} \beta_{ii} . X_i^2 + \sum_{i=1}^{2} \sum_{j=i+1}^{3} \beta_{ij} . X_i . X_j \quad (2)$$

Where; Y is the response variable; β_o is the constant, β_i, β_{ii}, and β_{ij} are coefficients; X_i, X_j are the independent variables. Subsequently, the optimum conditions for the biosynthesis of AgNPs were determined from the developed models using Excel Solver.

3. RESULTS AND DISCUSSION

3.1 Biosynthesis of AgNPs

Figures 1 and 2 present typical results from the biosynthesis of AgNPs using a 1.5 mM $AgNO_3$ solution, OPE concentration of 0.0075 g/mL, and pH of 11. The change of the solution color from yellowish to light brown within 15 to 30 min indicated the formation of nanoparticles (Figure 1). Similar findings have been reported in many studies (Jyoti and Singh, 2016; Saha et al., 2017). The change in color occurred due to the bioreduction of aqueous Ag^+ ions into AgNPs accompanied by SPR (Vanaja et al., 2014; Bonnia et al., 2016). In Figure 2, a plot of absorbance vs. wavelength shows the characteristic SPR wavelength peak for AgNPs at around 410 nm resulting in an intense change of color. Various experimental runs in CCD resulted in similar UV-vis spectra and exhibited a wide variation in peak absorbance and SPR wavelength. It has been reported that the SPR wavelength peak and width may be influenced by the changes in the size and shape of the nanoparticles (Evanoff and Chumanov, 2005; Wiley et al., 2006). In general, the size distributions of AgNPs based on the DLS analysis exhibited a unimodal peak (Figure 3) with average particle size in the range of 1-50 nm.

(a) (b)

Figure 1. Change in color of OPE after formation of colloidal AgNPs: (a) before; (b) after.

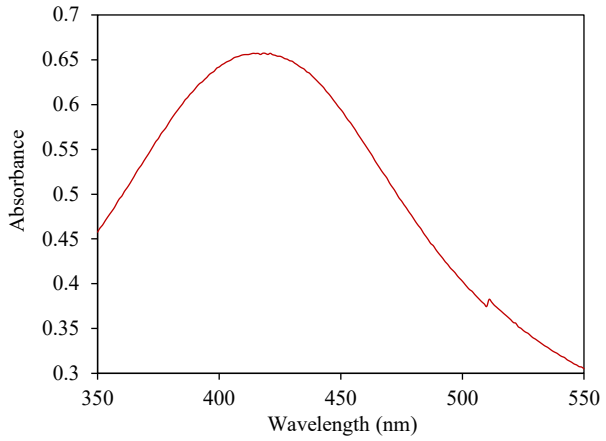

Figure 2. UV-visible absorbance spectrum of the biosynthesized AgNPs.

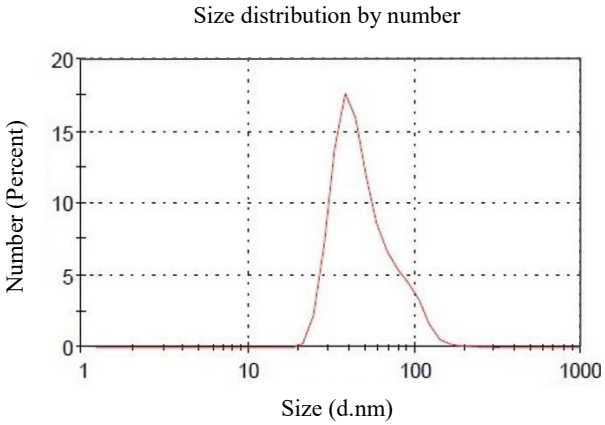

Figure 3. A typical plot of AgNPs size distribution from DLS (Malvern Zetasizer v7.02).

3.2 Models for biosynthesis of AgNPs based on CCD

Equations 3 to 5 present the regression models in coded units for the three response variables based on the experimental runs (Table 3). The coefficients of determination (R^2) for the developed models ranged from 0.735 to 0.923. The coefficients of the predictor terms in the developed models indicated their respective contributions for the estimation of response variables.

3.3 Model evaluation and optimization

Equations 3-5 indicated that among the indicator variables, pH had the most important effect on the biosynthesis of AgNPs. The contributions of interactions and quadratic terms were relatively small in all models. The influence of each independent variable on the normalized absorbance spectra was evaluated by considering its minimum and maximum values while keeping the other two independent variables at their mean values. An additional test in which all independent variables were set at their mean values was also included for comparison. Thus, sample nos. 9, 10, and 15 in Table 3 were selected for the OPE concentration. Figure 4 shows that a significant shift of SPR wavelength resulted towards red with a decrease in OPE concentration indicating the formation of larger AgNPs. In comparison, the change in normalized peak absorbance was relatively small.

The effect of pH on the biosynthesis of AgNPs (samples nos. 11, 12, and 15 in Table 3) is shown in Figure 5. A low pH of about 5.6 resulted in larger particle size and a higher pH of about 12.4 produced smaller AgNPs as indicated by the shift in SPR wavelength peaks (Figure 5). The pH has been reported to influence the size and shape of the AgNPs during biosynthesis due to the changes in binding and electrostatic repulsion ability of biomolecules present in the solution (Andreescu et al., 2007; Hasan et al., 2018) where high pH leads to the smaller nanoparticle sizes (Vanaja et al., 2014).

Likewise, the effect of $AgNO_3$ concentration was evaluated using sample nos. 13, 14, and 15 in Table 3 as shown in Figure 6. An increase in the $AgNO_3$ concentration resulted in a decrease of SPR wavelength from 438 to 430 nm and an increase in absorbance from 0.187 to 0.572 (Table 3), indicating the formation of smaller nanoparticles with a corresponding increase in their concentration.

The trends presented in Figures 4-6 and the corresponding experimental values in Table 3 indicate that increasing values of three process variables resulted in an increase in peak absorbance and a decrease in both SPR wavelength and nanoparticles size. Table 4 presents the optimum conditions for the biosynthesis of AgNPs as determined by the models (equations 3-5) resulting in maximum absorbance, minimum SPR wavelength and minimum particle size. The optimum conditions, based on overall considerations, included an OPE concentration of about 0.0075 g/mL, pH of 11 and $AgNO_3$ concentration of 1.5 mM for the biosynthesis of AgNPs to ensure maximum concentration of AgNPs based on the smallest particle size.

$$Y_1 = 0.432 + 0.067\,X_1 + 0.1178\,X_2 + 0.088\,X_3 - 0.0264\,X_1X_2 + 0.0246\,X_1X_3 + 0.0197X_2X_3 - 0.00057\,X_1^2 + 0.0461\,X_2^2 - 0.0064\,X_3^2 \quad (R^2=0.923) \quad (3)$$

$$Y_2 = 424.822 - 5.737\,X_1 - 8.849X_2 + 0.625X_3 + 0.25X_1X_2 + 0.75\,X_1X_3 + 0.75X_2X_3 - 2.996\,X_1^2 - 2.819X_2^2 + 1.2448\,X_3^2 \quad (R^2=0.735) \quad (4)$$

$$Y_3 = 32.0328 - 5.449\ X_1 - 14.59\ X_2 + 3.762\ X_3 - 0.444\ X_1X_2 - 5.637\ X_1X_3 + 1.720X_2X_3 + 4.282\ X_1^2 - 0.531\ X_2^2 - 2.249\ X_3^2 \quad (R^2=0.859) \quad (5)$$

Where; Y_1=peak absorbance, Y_2=SPR wavelength (nm), Y_3=AgNPs size (nm), X_1=OPE conc. (g/mL), X_2=pH, and X_3=$AgNO_3$ conc. (mM).

Table 3. Experimental and predicted values of response variables in biosynthesis of AgNPs.

Run No.	Coded variables			Absorbance		SPR wavelength (nm)		AgNPs size based on number (nm)	
	X_1	X_2	X_3	Expt.	Pred.	Expt.	Pred.	Expt.	Pred.
1	-1 -2.5	-1 -7	-1 -0.16	0.32	0.24	430	436	50.8	45.45
2	1 -7.5	-1 -11	-1 -1.5	0.34	0.33	414	422	46.19	46.71
3	-1 -2.5	1 -7	-1 -0.16	0.49	0.44	408	416	14.04	13.71
4	1 -7.5	1 -11	-1 -1.5	0.57	0.52	402	404	25.32	13.2
5	-1 -2.5	-1 -7	1 -0.16	0.33	0.33	428	434	48.43	60.81
6	1 -7.5	-1 -11	1 -1.5	0.53	0.52	424	424	38.93	39.52
7	-1 -2.5	1 -7	1 -0.16	0.66	0.61	418	418	36.21	35.95
8	1 -7.5	1 -11	1 -1.5	0.77	0.79	406	408	7.28	12.89
9	-1.68 -0.8	0 -9	0 -1	0.24	0.32	434	426	57.01	53.31
10	1.68 -9.2	0 -9	0 -1	0.55	0.55	410	407	31.64	34.98
11	0 -5	-1.68 -5.64	0 -1	0.34	0.37	440	432	59.78	55.07
12	0 -5	1.68 -12.4	0 -1	0.72	0.76	405	402	1.64	5.98
13	0 -5	0 -9	-1.68 -0.16	0.19	0.27	438	427	48.95	19.33
14	0 -5	0 -9	1.68 -1.84	0.57	0.57	430	429	42.76	31.99
15	0 -5	0 -9	0 -1	0.48	0.43	422	425	28.75	32.03
16	0 -5	0 -9	0 -1	0.46	0.43	415	425	33.26	32.03
17	0 -5	0 -9	0 -1	0.39	0.43	431	425	32.41	32.03
18	0 -5	0 -9	0 -1	0.43	0.43	425	425	29.44	32.03
19	0 -5	0 -9	0 -1	0.42	0.43	425	425	35.95	32.03
20	0 -5	0 -9	0 -1	0.44	0.43	429	425	32.3	32.03

*X_1 (mg/mL)=OPE conc.; X_2=pH; X_3=$AgNO_3$ conc. Actual values are shown in parentheses.

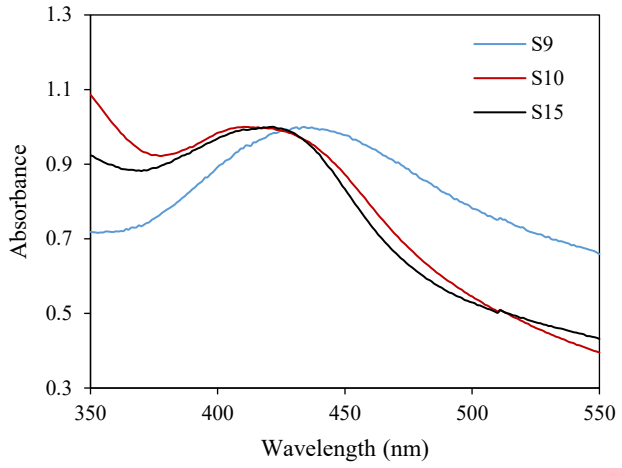

Figure 4. Absorbance spectra of AgNPs biosynthesized with different OPE concentration.

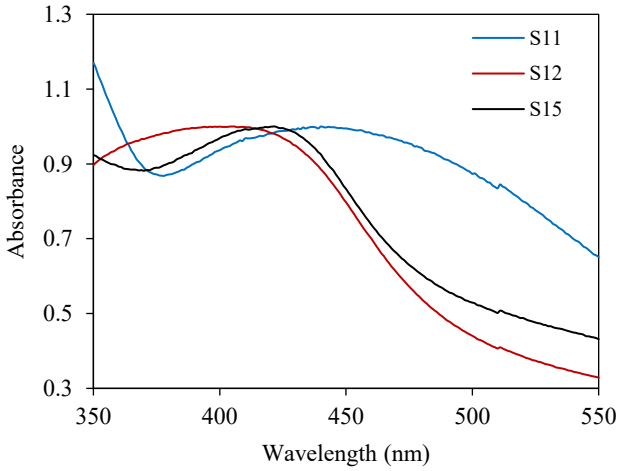

Figure 5. Absorbance spectra of AgNPs biosynthesized with different pH.

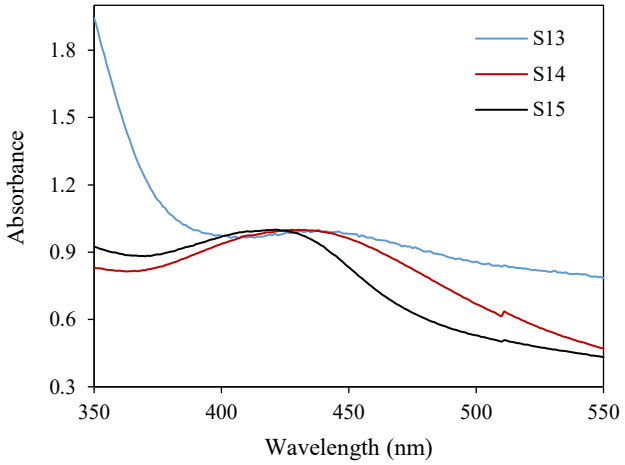

Figure 6. Absorbance spectra of AgNPs biosynthesized with different $AgNO_3$ concentration.

The optimum conditions for the biosynthesis of AgNPs using OPE reported in the literature are in the range of 1-4 mM $AgNO_3$ concentration and 4.5-9 pH to form particle sizes in 5- 46 nm range (Basavegowda and Lee, 2013; Kahrilas et al., 2014; De Barros Santos et al., 2015; Dutta et al., 2020; Saratale et al., 2018). The results obtained in this study (Table 4) appear to agree with the past studies and correspond to the smallest size of AgNPs and maximum concentration in solution.

3.4 Surface plots for particle size and peak absorbance for biosynthesis of AgNPs

The plot in Figure 7(a) shows peak absorbance as a function of OPE concentration and pH, with $AgNO_3$ concentration held constant at the mean value for AgNPs biosynthesis. An increase in both OPE concentration and pH resulted in an increase in the peak absorbance of AgNPs solution in the respective ranges of the experimental variables. Similar trends for the variation in peak absorbance were also observed in Figure 7(b) and Figure 7(c) for the effect of $AgNO_3$ concentration and pH, and $AgNO_3$ and OPE concentrations, respectively.

Table 4. Optimum conditions for the biosynthesis of AgNPs.

Response variable	Coded and actual values			Optimum value
	X_1	X_2	X_3	
Absorbance	1 (0.0075)	1 (11)	1 (1.5)	0.79
SPR wavelength (nm)	1 (0.0075)	1 (11)	-0.854 0.427	403.8
Mean particle size (nm)	1 (0.0075)	1 (11)	1 (1.5)	12.89

Figure 8 presents the effects of OPE concentration, pH and $AgNO_3$ concentration on the average size of AgNPs. The smallest particle size was produced at higher pH in combination with lower concentrations of OPE or $AgNO_3$ as shown in Figure 8 (a) and Figure 8 (b), respectively. However, lower concentrations of $AgNO_3$ and higher concentrations of OPE resulted in smaller nanoparticles size as shown in Figure 8 (c). The surface plots in Figures 7 and 8 clearly indicate that the process variables followed identical trends resulting in maximum absorbance and minimum nanoparticle size, respectively.

3.5 Relationship between peak absorbance, SPR wavelength and AgNPs size

Figures 9 and 10 present the mean size of biosynthesized AgNPs as a function of peak absorbance and SPR wavelength, respectively. As

observed in Figures 9 and 10, a decrease in peak absorbance in association with an increase in the particle size or an increase in the SPR wavelength has been similarly reported in the literature (Gupta et al., 2002; Fleger and Rosenbluh, 2009). Thus a red-shift in SPR wavelength in UV-vis spectra indicates an increase in the size of AgNPs. Many empirical relationships for estimating the size of gold and AgNPs in colloidal suspension have been proposed for fast and easy characterization (Haiss et al., 2007; Ashkarran and Bayat, 2013; Dalal et al., 2019).

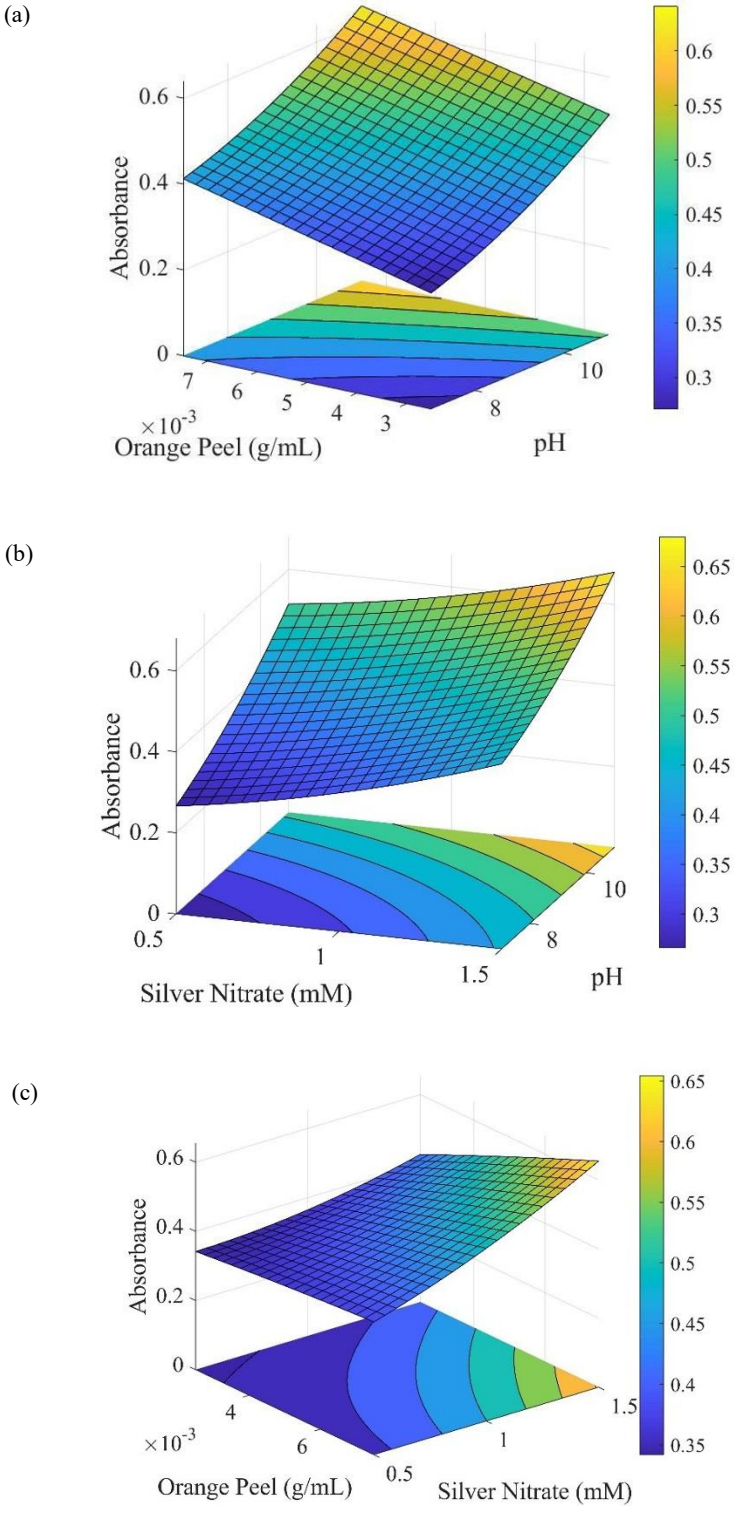

Figure 7. Surface plots showing absorbance as a function of OPE concentration and pH (a), $AgNO_3$ concentration and pH (b), and OPE concentration and $AgNO_3$ concentration (c).

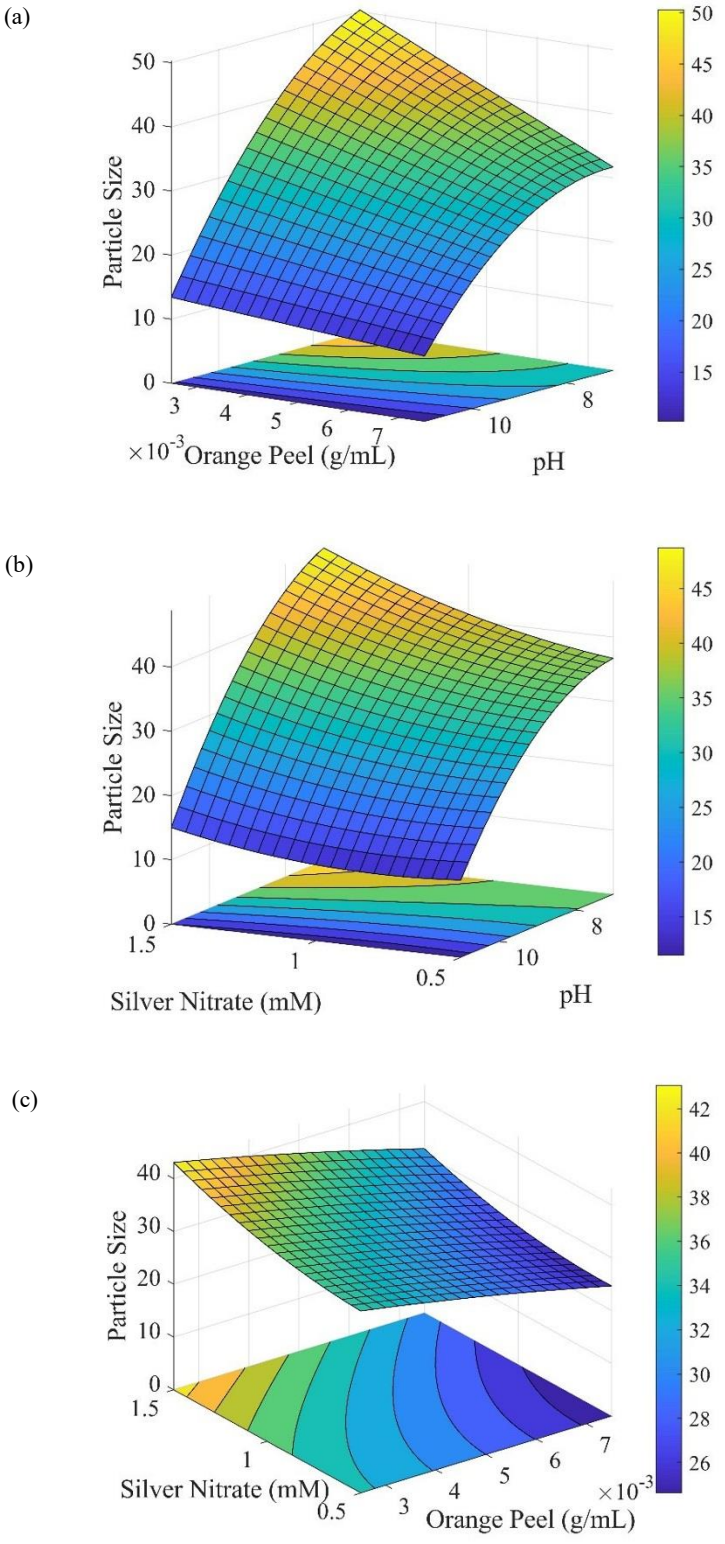

Figure 8. Surface plots showing AgNPs size as a function of OPE concentration and pH (a), $AgNO_3$ concentration and pH (b), and OPE concentration and $AgNO_3$ concentration (c).

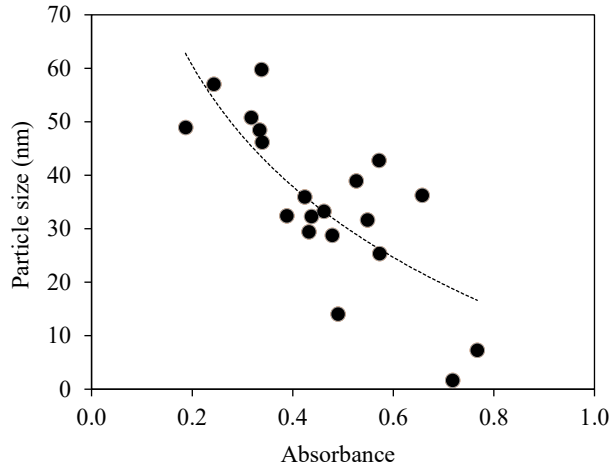

Figure 9. Relationship between AgNPs size and peak absorbance in UV-vis spectra.

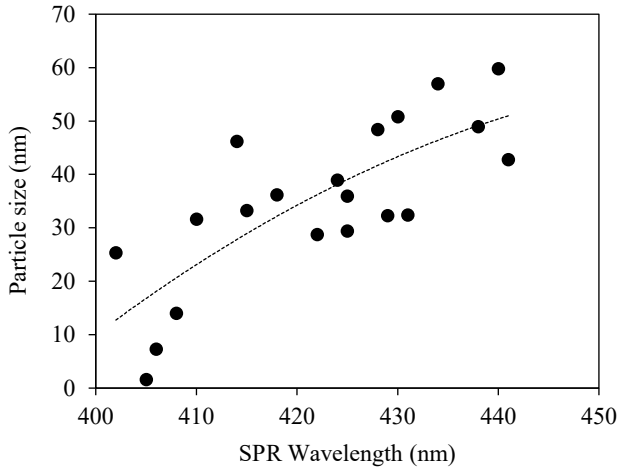

Figure 10. Relationship between AgNPs size and SPR wavelength in UV-vis spectra

3.6 Effect of AgNPs on MB dye reduction

There are many studies on the reduction of MB dye by $NaBH_4$ in the presence of AgNPs. However, the information on the relative significance of the individual concentrations of MB dye, $NaBH_4$ and AgNPs in catalytic dye reduction is not available.

Table 5 presents the results from a full-factorial experimental design for MB dye degradation by $NaBH_4$ and AgNPs. The following relationship was developed in coded units using Equation 2 without the inclusion of quadratic terms.

$$\text{Dye degradation (\%)} = 93.70 + 2.357\,X_1 - 2.822\,X_2 - 0.146\,X_3 + 1.874\,X_1X_2 + 0.920\,X_1X_3 - 0.352\,X_2X_3 \quad (R^2 = 0.89) \quad (6)$$

The coefficients in the fitted model (Equation 6) indicate the independent contributions of the main factors and their interactions in MB dye degradation and can be ranked from high to low as follows.

$$X_2 > X_1 > X_1X_2 > X_1X_3 > X_2X_3 > X_3$$

These results showed that AgNPs (X_2) contributed the most to catalytic MB dye degradation, followed by dye concentration (X_1) and their interactions (X_1X_2 and X_1X_3). In contrast, $NaBH_4$ (X_3) contributed the least with minor effects of its interaction with AgNPs (X_2) and dye concentration (X_1).

Figure 11 shows the pictorial view of MB dye degradation in 20 mL vials with an initial concentration of 0.5 mM in the presence of 1 mM $NaBH_4$ and 1 mL AgNPs solution. The MB dye changed from its natural state dark color to light blue in the first 5 min and turned light yellowish after about 50 min. However, the MB dye degradation without $NaBH_4$ under similar conditions showed only a slight visible change in the color of the MB dye even after a 180 min reaction time without AgNPs (Figure 12).

Table 5. Catalytic reduction of MB in presence of $NaBH_4$ and AgNPs.

RUN	Code			A_0	A_t=60 min	MB dye degradation	
	X_1	X_2	X_3			Expt. (%).	Pred. (%).
1	-1 (0.0319)	-1 (1)	-1 (0.1)	0.22	0.01	95.45	96.78
2	1 (0.319)	-1 (1)	-1 (0.1)	3.048	0.12	96.06	95.91
3	-1 (0.03190	1 (1)	-1 (0.1)	0.288	0.034	88.19	88.04
4	1 (0.319)	1 (1)	-1 (0.1)	2.115	0.141	93.33	94.66

*X_1(mg/mL) = MB dye conc.; X_2 = AgNPs; X_3 = $NaBH_4$ conc.

Table 5. Catalytic reduction of MB in presence of $NaBH_4$ and AgNPs (cont.).

RUN	Code			A_0	A_t=60 min	MB dye degradation	
	X_1	X_2	X_3			Expt. (%).	Pred. (%).
5	-1 (0.0319)	-1 (1)	1 (0.9)	0.264	0.012	95.45	95.3
6	1 (0.319)	-1 (1)	1 (0.9)	2.793	0.09	96.78	98.11
7	-1 (0.0319)	1 (10)	1 (0.9)	0.224	0.036	83.93	85.26
8	1 (0.319)	1 (10)	1 (0.9)	2.987	0.128	95.71	95.56
9	0 (0.1759)	0 (5.5)	0 (0.5)	1.651	0.067	95.94	93.7
10	0 (0.1759)	0 (5.5)	0 (0.5)	1.721	0.066	96.17	93.7

*X_1(mg/mL) = MB dye conc.; X_2 = AgNPs; X_3 = $NaBH_4$ conc.

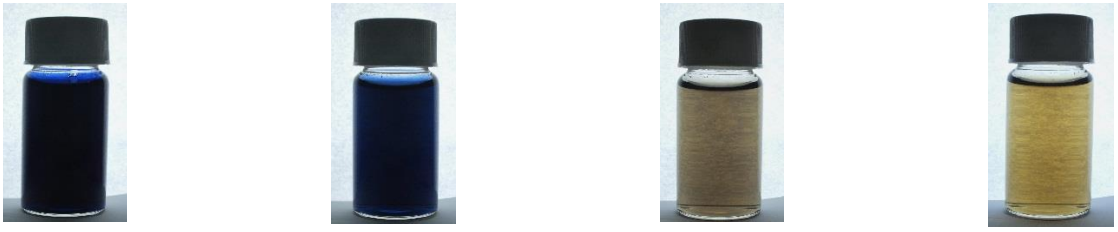

t=0 min t=5 min t=20 min t=50 min

Figure 11. Change in color during MB dye degradation in presence of $NaBH_4$.

t=0 min t=5 min t=30 min t=180 min

Figure 12. Change in color during MB dye degradation in absence of $NaBH_4$.

The pictorial trends for dye degradation in Figures 11 and 12 are presented quantitatively in Figure 13. Though there was a sharp reduction in dye concentration initially when using the AgNPs alone, the addition of $NaBH_4$ further expedited the dye reduction process.

A rapid degradation of MB dye within 2-10 min has been reported with the addition of AgNPs in a mixture of MB dye and $NaBH_4$ (Indana et al., 2016; Saha et al., 2017). On the other hand, longer times were needed for MB dye degradation in the absence of $NaBH_4$ (Santhanalakshmi and Venkatesan, 2011; Vanaja et al., 2014). Several studies have indicated that catalytic degradation of MB dye takes place at the surface of AgNPs (Vidhu and Philip, 2014; Jyoti and Singh, 2016; Saha et al., 2017). AgNPs act as an efficient catalyst through the electron transfer between $NaBH_4$ acting as a donor and MB dye as acceptor. Thus, the reduction of MB dye by $NaBH_4$ increases in the presence of AgNPs. In addition, the smaller size of AgNPs may promote the catalytic activity due to the availability of large surface area (Suvith and Philip, 2014; Bonnia et al., 2016).

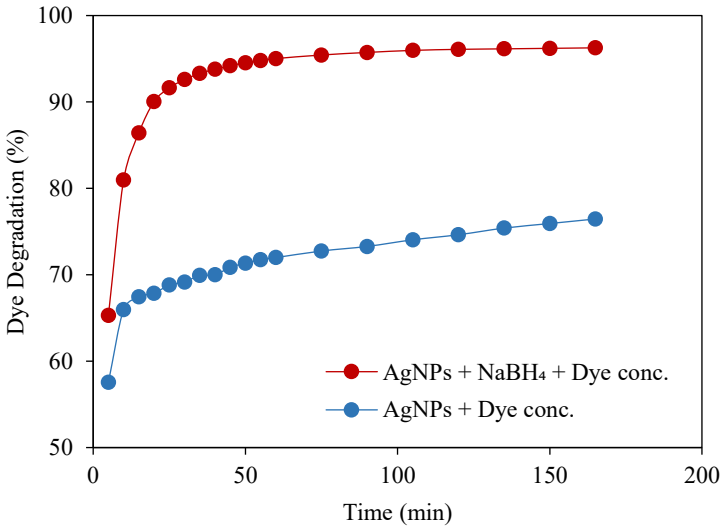

Figure 13. Catalytic MB dye degradation with time in presence of AgNPs and $NaBH_4$.

4. CONCLUSION

The biosynthesis of AgNPs could be carried out using OPE without requiring toxic chemicals. Models based on the CCD in RSM identified the effects of OPE concentration, pH and $AgNO_3$ concentration on the peak absorbance and SPR wavelength in UV-vis spectra, and particle size as response variables. The pH had the maximum influence on the formation of AgNPs compared to the OPE and $AgNO_3$ concentration. The optimum conditions (OPE concentration of 0.0075 g/mL, pH of 11 and $AgNO_3$ concentration of 1.5 mM) resulted in the mean particle size, SPR wavelength and absorbance of about 12.9 nm, 403.8 nm and 0.79, respectively. AgNPs had a major influence on the MB dye degradation compared to the initial dye concentration and $NaBH_4$. This was confirmed by the quick discoloration of MB dye by AgNPs alone and in combination with $NaBH_4$. Results showed that AgNPs biosynthesized by OPE offer an inexpensive and eco-friendly treatment method for catalytic reduction of MB dye in industrial effluent.

ACKNOWLEDGEMENTS

The authors would like to express their sincere appreciation to the Department of Civil and Environmental Engineering, Faculty of Engineering, Mahidol University, Salaya campus for making available the laboratory facilities.

REFERENCES

Ahmad S, Munir S, Zeb N, Ullah A, Khan B, Ali J, et al. Green nanotechnology: A review on green synthesis of silver nanoparticles - an ecofriendly approach. International Journal of Nanomedicine 2019;14:5087-107.

Andreescu D, Eastman C, Balantrapu K, Goia DV. A simple route for manufacturing highly dispersed silver nanoparticles. Journal of Materials Research 2007;22(9):2488-96.

Ashkarran AA, Bayat A. Surface plasmon resonance of metal nanostructures as a complementary technique for microscopic size measurement. International Nano Letters 2013;3:50.

Basavegowda N, Lee YR. Synthesis of silver nanoparticles using Satsuma mandarin (*Citrus unshiu*) peel extract: A novel approach towards waste utilization. Materials Letters 2013; 109:31-3.

Bátori V, Jabbari M, Åkesson D, Lennartsson PR, Taherzadeh MJ, Zamani A. Production of pectin-cellulose biofilms: A new approach for citrus waste recycling. International Journal of Polymer Science 2017;2017:9732329.

Bhakya S, Muthukrishnan S, Sukumaran M, Muthukumar M, Kumar ST, Rao MV. Catalytic degradation of organic dyes using synthesized silver nanoparticles: A green approach. Journal of Bioremediation and Biodegredation 2015;6(5): 1000312.

Bhattarai B, Zaker Y, Bigioni TP. Green synthesis of gold and silver nanoparticles: Challenges and opportunities. Current Opinion in Green and Sustainable Chemistry 2018;12:91-100.

Biswas S, Mulaba-Bafubiandi AF. Optimization of process variables for the biosynthesis of silver nanoparticles by *Aspergillus wentii* using statistical experimental design. Advances in Natural Sciences: Nanoscience and Nano-technology 2016;7(4):045005.

Bonnia NN, Kamaruddin MS, Nawawi MH, Ratim S, Azlina HN, Ali ES. Green biosynthesis of silver nanoparticles using 'Polygonum Hydropiper' and study its catalytic degradation of methylene blue. Procedia Chemistry 2016;19:594-602.

Chinnasamy C, Tamilselvam P, Karthik V, Karthick B. Optimization, and characterization studies on green synthesis of silver nanoparticles using response surface methodology. Advances in Natural and Applied Sciences 2017;11(4): 214-22.

Dalal N, Boruah BS, Neoh A, Biswas R. Correlation of surface plasmon resonance wavelength (SPR) with size and

concentration of noble metal nanoparticles. Annals of Reviews and Research 2019;5(2):555658.

De Barros Santos E, Madalossi NV, Sigoli FA, Mazali IO. Silver nanoparticles: Green synthesis, self-assembled nanostructures, and their application as SERS substrates. New Journal of Chemistry 2015;39(4):2839-46.

Dutta T, Chattopadhyay AP, Ghosh NN, Khatua S, Acharya K, Kundu S, et al. Biogenic silver nanoparticle synthesis and stabilization for apoptotic activity; insights from experimental and theoretical studies. Chemical Papers 2020;74:4089-101.

Evanoff Jr DD, Chumanov G. Synthesis and optical properties of silver nanoparticles and arrays. ChemPhysChem 2005;6(7): 1221-31.

Fleger Y, Rosenbluh M. Surface plasmons and surface enhanced Raman spectra of aggregated and alloyed gold-silver nanoparticles. Research Letters in Optics 2009;2009:475941.

Gupta R, Dyer MJ, Weimer WA. Preparation and characterization of surface plasmon resonance tunable gold and silver films. Journal of Applied Physics 2002;92(9):5264-71.

Gupta M, Gularıa P, Sıngh D, Gupta S. Analysis of aroma active constituents, antioxidant, and antimicrobial activity of *C. sinensis*, *Citrus limetta* and *C. limon* fruit peel oil by GC-MS. Biosclences Biotechnology Research Asia 2014;11(2):895-9.

Haiss W, Thanh NT, Aveyard J, Fernig DG. Determination of size and concentration of gold nanoparticles from UV-Vis spectra. Analytical Chemistry 2007;79(11):4215-21.

Hasan M, Ullah I, Zulfiqar H, Naeem K, Iqbal A, Gul H, et al. Biological entities as chemical reactors for synthesis of nanomaterials: Progress, challenges, and future perspective. Materials Today Chemistry 2018;8:13-28.

Heydari S, Zaryabi MH. Response surface methodology for optimization of green silver nanoparticles synthesized via *Phlomis cancellata* bunge extract. Analytical and Bioanalytical Chemistry Research 2018;5(2):373-86.

Husain Q. Peroxidase mediated decolorization and remediation of wastewater containing industrial dyes: A review. Reviews in Environmental Science and Bio/Technology 2010;9(2):117-40.

Indana MK, Gangapuram BR, Dadigala R, Bandi R, Guttena V. A novel green synthesis and characterization of silver nanoparticles using gum tragacanth and evaluation of their potential catalytic reduction activities with methylene blue and Congo red dyes. Journal of Analytical Science and Technology 2016;7(1):1-9.

Jana NR, Wang ZL, Pal T. Redox catalytic properties of palladium nanoparticles: Surfactant and electron donor-acceptor effects. Langmuir 2000;16(6):2457-63.

Jamkhande PG, Ghule NW, Bamer AH, Kalaskar MG. Metal nanoparticles synthesis: An overview on methods of preparation, advantages and disadvantages, and applications. Journal of Drug Delivery Science and Technology 2019; 53:101174.

Jyoti K, Singh A. Green synthesis of nanostructured silver particles and their catalytic application in dye degradation. Journal of Genetic Engineering and Biotechnology 2016; 14(2):311-7.

Kahrilas GA, Wally LM, Fredrick SJ, Hiskey M, Prieto AL, Owens JE. Microwave-assisted green synthesis of silver nanoparticles using orange peel extract. ACS Sustainable Chemistry and Engineering 2014;2(3):367-76.

Kaviya S, Santhanalakshmi J, Viswanathan B, Muthumary J, Srinivasan K. Biosynthesis of silver nanoparticles using citrus sinensis peel extract and its antibacterial activity. Spectrochimica Acta Part A: Molecular and Biomolecular Spectroscopy 2011;79(3):594-8.

Khodadadi B, Bordbar M, Nasrollahzadeh M. *Achillea millefolium* L. extract mediated green synthesis of waste peach kernel shell supported silver nanoparticles: Application of the nanoparticles for catalytic reduction of a variety of dyes in water. Journal of Colloid and Interface Science 2017;493:85-93.

Menon S, KS SD, Agarwal H, Shanmugam VK. Efficacy of biogenic selenium nanoparticles from an extract of ginger towards evaluation on anti-microbial and antioxidant activities. Colloid and Interface Science Communications 2019;29:1-8.

Nasuha N, Hameed BH, Din AT. Rejected tea as a potential low-cost adsorbent for the removal of methylene blue. Journal of Hazardous Materials 2010;175(1-3):126-32.

Ndolomingo MJ, Bingwa N, Meijboom R. Review of supported metal nanoparticles: Synthesis methodologies, advantages, and application as catalysts. Journal of Materials Science 2020;55(15):6195-241.

Nikaeen G, Yousefinejad S, Rahmdel S, Samari F, Mahdavinia S. Central composite design for optimizing the biosynthesis of silver nanoparticles using plantago major extract and investigating antibacterial, antifungal and antioxidant activity. Scientific Reports 2020;10(1):1-6.

Ozturk B, Parkinson C, Gonzalez-Miquel M. Extraction of polyphenolic antioxidants from orange peel waste using deep eutectic solvents. Separation and Purification Technology 2018;206:1-13.

Patil RS, Kokate MR, Kolekar SS. Bioinspired synthesis of highly stabilized silver nanoparticles using *Ocimum tenuiflorum* leaf extract and their antibacterial activity. Spectrochimica Acta Part A: Molecular and Biomolecular Spectroscopy 2012; 91:234-8.

Raj S, Singh H, Trivedi R, Soni V. Biogenic synthesis of AgNPs employing *Terminalia arjuna* leaf extract and its efficacy towards catalytic degradation of organic dyes. Scientific Reports 2020;10:9616.

Rostami-Vartooni A, Nasrollahzadeh M, Alizadeh M. Green synthesis of seashell supported silver nanoparticles using *Bunium persicum* seeds extract: Application of the particles for catalytic reduction of organic dyes. Journal of Colloid and Interface Science 2016;470:268-75.

Sabouri MR, Sohrabi MR, Moghaddam AZ. A novel and efficient dyes degradation using bentonite supported zero-valent iron-based nanocomposites. Chemistry Select 2020;5(1):369-78.

Saha J, Begum A, Mukherjee A, Kumar S. A novel green synthesis of silver nanoparticles and their catalytic action in reduction of methylene blue dye. Sustainable Environment Research 2017; 27(5):245-50.

Santhanalakshmi J, Venkatesan P. Mono and bimetallic nanoparticles of gold, silver and palladium-catalyzed NADH oxidation-coupled reduction of Eosin-Y. Journal of Nanoparticle Research 2011;13(2):479-90.

Saratale RG, Shin HS, Kumar G, Benelli G, Ghodake GS, Jiang YY, et al. Exploiting fruit byproducts for eco-friendly nanosynthesis: *Citrus* × *clementina* peel extract mediated fabrication of silver nanoparticles with high efficacy against microbial pathogens and rat glial tumor C6 cells. Environmental Science and Pollution Research 2018; 25(11):10250-63.

Sethpakdee R. Citrus production in Thailand. Taipei: Food and Fertilizer Technology Center; Extension Bulletin No. 437 [Internet]. 1997 [cited 2021 Jan 20]. Available from: http://swfrec.ifas.ufl.edu/hlb/database/pdf/00001303.pdf.

Shanmuganathan R, Karuppusamy I, Saravanan M, Muthukumar H, Ponnuchamy K, Ramkumar VS, et al. Synthesis of silver nanoparticles and their biomedical applications: A comprehensive review. Current Pharmaceutical Design 2019; 25(24):2650-60.

Suvith VS, Philip D. Catalytic degradation of methylene blue using biosynthesized gold and silver nanoparticles. Spectrochimica Acta Part A: Molecular and Biomolecular Spectroscopy 2014;118:526-32.

Vanaja M, Paulkumar K, Baburaja M, Rajeshkumar S, Gnanajobitha G, Malarkodi C, et al. Degradation of methylene blue using biologically synthesized silver nanoparticles. Bioinorganic Chemistry and Applications 2014;2014:742346.

Vidhu VK, Philip D. Catalytic degradation of organic dyes using biosynthesized silver nanoparticles. Micron 2014;56:54-62.

Wiley BJ, Im SH, Li ZY, McLellan J, Siekkinen A, Xia Y. Maneuvering the surface plasmon resonance of silver nanostructures through shape-controlled synthesis. Journal of Physical Chemistry B 2006;110(32):15666-75.

Xu L, Wang YY, Huang J, Chen CY, Wang ZX, Xie H. Silver nanoparticles: Synthesis, medical applications, and biosafety. Theranostics 2020;10(20):8996-9031.

Zhang D, Ma XL, Gu Y, Huang H, Zhang GW. Green synthesis of metallic nanoparticles and their potential applications to treat cancer. Frontiers in Chemistry 2020;8:799.

Zollinger H. Color Chemistry: Syntheses, Properties, and Applications of Organic Dyes and Pigments. New York, USA: Wiley-VCH; 1987.